COMMUNICATIONS IN COMPUTATIONAL PHYSICS
Vol. **4**, No. 5, pp. 1258-1278

Commun. Comput. Phys.
November 2008

# Simulation of High Power THz Emission from Laser Interaction with Tenuous Plasma and Gas Targets†

Zheng-Ming Sheng[1,2,*], Hui-Chun Wu[3], Wei-Min Wang[2], Min Chen[2], Xiao-Gang Dong[2], Jun Zheng[1] and Jie Zhang[1,2]

[1] *Department of Physics, Shanghai Jiao Tong University, Shanghai 200240, China.*
[2] *Beijing National Laboratory for Condensed Matter Physics, Institute of Physics, CAS, Beijing 100190, China.*
[3] *Max-Planck-Institut für Quanenoptik, D-85748 Garching, Germany.*

Received 28 March 2008; Accepted (in revised version) 3 September 2008

Communicated by Zhihong Lin

Available online 9 September 2008

**Abstract.** With one- and two-dimensional particle-in-cell (PIC) codes, we simulate the generation of high power terahertz (THz) emission from the interaction of ultrashort intense lasers with tenuous plasma and gas targets. By driving high-amplitude electron plasma waves either with a laser wakefield or the beatwave of two laser pulses, powerful THz electromagnetic pulses can be produced by linear mode conversion in inhomogeneous plasma or by the transient current induced at the surfaces of a thin plasma layer of few plasma wavelengths. Even with incident lasers at moderate intensity such as $10^{17}W/cm^2$, the produced emission can be at the level of tens of MW in power and capable of affording field strengths of a few MV/cm, suitable for the studies of THz nonlinear physics. With field ionization included in the PIC codes, THz emission from laser interaction with tenuous gas targets is simulated. It is found that the transient transverse current formed during the ionization processes is responsible for the THz emission. With this mechanism, one may also obtain THz fields of MV/cm at lower laser intensity as compared with the schemes of plasma-wave excitation.

**AMS subject classifications**: 78A40, 78M25, 81V10

**Key words**: Particle-in-cell simulation, laser-plasma, electron plasma wave, high power THz emission.

†Dedicated to Professor Xiantu He on the occasion of his 70th birthday.

*Corresponding author. *Email address:* zmsheng@sjtu.edu.cn (Sheng), hcwu@mpq.mpg.de (Wu), hbwwm1@aphy.iphy.ac.cn (Wang), mchen@tp1.uni-duesseldorf.de (Chen), xgdong@aphy.iphy.ac.cn (Dong), jzheng@sjtu.edu.cn (Zheng), jzhang1@sjtu.edu.cn (Zhang)

 

# 1 Introduction

The recent development of laser technologies has enabled one to obtain ultrashort high power laser pulses with pulse duration ranging from few femtoseconds (or few cycles) to picosecond, peak power ranging from terawatt to the petawatt level, and focused intensity over $10^{20}W/cm^2$ [1]. The future development shall allow one to access even extreme laser conditions. Apparently such lasers provide countless possibilities of applications, such as laser fusion [2], creation of high energy density states [3, 4], advanced electron accelerators [5], energetic ion beams [6, 7], and novel radiation sources [8, 9]. For the last ones, currently the terahertz radiation (1THz=$10^{12}$Hz) from laser irradiated targets is attracting increasing interest. THz science and Technology become a frontier of research for intercrossing disciplines covering physics, chemistry, biology, materials science, and medicine now [10–13]. The THz radiation usually means the gap in the electromagnetic spectrum from 0.3 to 20 THz (1mm to 15$\mu m$ in wavelength), which was not conventionally accessible either with optical methods or with electronical methods. However, the situation changes with the use of ultrashort laser pulses because their spectrum width (the inverse of the pulse duration) can be made in the THz regime. Currently based upon the optical schemes it is found that THz emission can be generated by optical rectification, optical conductive antenna, nonlinear difference frequency mixing, tunable parametric oscillators, optical Cherenkov radiation, etc. However, due to the damage limit of the optical materials, one cannot irradiate these optical materials with very high power lasers. With these schemes, it is thus difficult to obtain high power THz emission at the megawatt (MW) level. The latter is important for many applications and may allow one to study high-field and nonlinear physics in the THz regime in semiconductors, insulators, superconductors etc. [10] Currently MW narrow-band THz sources have been obtained from free electron lasers. Broad-band THz sources from ultrashort electron bunches either from linac and from laser wakefields are also suggested [14, 15].

On the other hand, plasma as a nonlinear optical media does not have a damage limit by high power lasers. Thus by irradiating plasma with such laser pulses, in principle one can obtain very high power THz pulses. Actually in 1990's, Hamster et al. observed experimentally THz emission by irradiating ultrashort laser pulses of 100 fs onto solid and gas targets [16]. Later THz emission from Cherenkov wakes in magnetized plasmas driven by ultrashort laser pulses was proposed [17, 18]. Recently, we suggested a new mechanism for THz emission based on the excitation of laser wakefields [19–23]. This emission is produced through linear mode conversion from a high-amplitude laser wakefield driven in inhomogeneous plasmas. This scheme can provide tens of megawatt (MW)-level emission with field amplitudes up to a few GV/m and still it allows for both compactness and relatively high efficiency by use of terawatt ultrashort laser pulses. Furthermore it is suggested that single-cycle THz emission can be produced with thin underdense plasma layers of few THz wavelengths in thickness irradiated by laser pulses [24].

In addition, ionizing gas targets are also potentially high power THz sources when irradiated by laser pulses at moderate intensities such as $10^{15-16}W/cm^2$ [25–31]. It is found

experimentally that THz emission can be produced either with single or two laser pulses. For example, laser filaments have been observed to emit electromagnetic radiation in the sub-THz region. Both transverse and very directional forward and backward emissions have been observed. There are several different explanations for these observed emissions, such as the four-wave mixing [25, 28], the oscillation of electrons in the plasma channel driven by the pondermotive force of the laser pulses [32], ionization-induced current models [33,34], Cherenkov emission from the ionization front moving faster than the speed of light in the medium [35], transition-Cherenkov emission from the plasma space charge moving behind the ionization front [36], transmission lines of neighboring laser filaments [37], etc. Up to now, however, these theoretical models are mostly qualitative. In order to explain the experimental results completely, quantitative comparison with experimental results is still required, where suitable numerical simulation is indispensable.

In this paper, we give a brief report on our recent simulation on THz emission from laser interaction with tenuous plasma and gas targets. In Section 2, a brief description of the numerical simulation codes used in our studies is given. In Section 3, two mechanisms of THz emission from laser interaction with tenuous plasmas are discussed. In Section 4, THz emission from gas targets irradiated by laser pulses at moderate intensity by field ionization processes is simulated and analyzed. A summary is given in Section 5.

## 2 Description of the particle-in-cell code with field ionization and particle collisions included

When a target is irradiated by an ultrashort intense laser pulse, usually strong kinetic effects, high nonlinearities, and several different physical processes are involved. The thermal equilibrium cannot be established in short time by collisions between particles and the fluid description usually fails to apply. In some case, one is particularly interested in the kinetic features of minority particles, such as the plasma wave-breaking, electron injection and trapping in the laser wakefields in underdense plasma [5], trapping and acceleration of protons by electrostatic collisionless shock waves in overdense plasma [38], transport of fast electrons in overdense plasma in the fast ignition scheme of fusion targets [39], etc. For such problems, kinetic simulation is necessary. The particle-in-cell (PIC) simulation is known to be able to deal with these kinetic effects effectively and it becomes a well-established tool for kinetic simulations in plasma physics and astrophysics [40–42] as compared with other kinetic schemes such as the Fokker-Planck and Vlasov schemes. We have been developing a parallelized PIC code KLAP (Kinetic LAser Plasmas) in one, two, and three-dimensional space for studying high intensity laser-matter interactions with field ionization and binary collisions between particles included [43].

In a PIC code, each particle is actually a macro-particle, which is a homogeneous collection of a large number of real-particles, either to be electrons, ions, or neutral atoms.

The large number of particles in plasma or unionized materials is replaced by a much smaller number of these macro-particles with its charge to mass ratio remains the same as that of the real particles. These particles have a finite size about a mesh in the discretized coordinate space. In the code, Maxwell's equations and the equations of motion for particles are solved self-consistently. Electric and magnetic fields, current and charge densities are defined at spatial grid points, while particles can take arbitrary positions. Electromagnetic fields at a position of a particle are interpolated from those at adjacent grid points. On the other hand, the current density and charge density at each grid point are computed from velocities and positions of charged particles. For the equations of motion, a time-centered Leap-Frog scheme is used according to Birdsall and Langdon [41], which allows for an accuracy of $\mathcal{O}(\Delta t^2)$. Charge and current assignments can be done locally with exact charge conservation [44, 45], which allows one to solve the Maxwell's equation without solving Poisson's equation at every time step. The Mawell's equation is usually solved with the finite difference time domain (FDTD) method with the absorption boundaries such as given in [46] or PML absorption boundaries [47]. Recently, a new scheme "Numerical Dispersion Free Maxwell Solver" is proposed by Sentoku [48], which is also a local solver and it is numerical dispersion free scheme for propagating wave along the grids. Also it is not necessary any more to introduce absorption boundaries with this scheme.

For the one-dimensional (1D) PIC code, in order to deal with the problem of oblique incidence of laser pulses, it is necessary to adopt a boosting frame method following Bourdier [49, 50]. One performs Lorentz transformation from the laboratory frame to a moving frame, which moves in the plane of incidence parallel to the plasma surface such that the laser pulse is normally incident to the target in the moving frame.

We have included the field ionization of atoms in the PIC code. It is assumed that the tunneling ionization is dominant in the high laser fields. The well-known ADK model for the ionization rate is adopted [51]. In each integration step $\Delta t$, firstly one calculates the ionization probability

$$P_{opt} = 1 - \exp\{-W_i[E(t)]\Delta t\},$$

where $W_i$ is the ionization rate at the field strength $E(t)$. Secondly, one generates a random number $q$ within [0,1]. If $q \leq P_{opt}$, field ionization occurs and an electron and an ion are born with zero velocities initially. For high order ionization, it is treated in the same way except the velocities of new born electrons which are the same as the ones of the mother ions. To account for the field energy loss during the ionization processes, a virtual ionization current is introduced:

$$\mathbf{J}_{ion} = \mathbf{E}(t)\sum_i \Delta n_{ei}(\epsilon_i + \epsilon_{ki}) / (\Delta t |\mathbf{E}(t)|^2),$$

where $\Delta n_{ei}$ is the electron density from the ions with charge $i$, $\epsilon_i$ is the ionization energy, and $\epsilon_{ki}$ is the initial kinetic energy of new-born electrons, which is usually close to their mother ions, much smaller than the quiver energy of electrons in the laser fields.

This ionization current is added to the real currents in the integration of the Maxwell's equations.

If the target density is high, with the increase of plasma density during the field ionization processes, the impact ionization becomes comparable to the field ionization, one need to take into account the impact ionization by electrons. A procedure similar to that given by Vahedi and Surendra [52] is adopted in our code. In addition, binary collision between particles can also be included in the PIC code with the scheme proposed by Takizuba and Abe [53], where elastic collisions are assumed. This scheme is extended further to the case when the particles move with relativistic speeds [54].

## 3 THz emission from tenuous plasmas irradiated by short intense laser pulses

It is well-known that a short intense laser propagating in underdense plasma can efficiently excite a high-amplitude electron plasma wave, which is also called the laser wakefield, provided the laser pulse duration is comparable to the electron plasma oscillation period. The latter is given by $T_p = 2\pi/\omega_p$, where $\omega_p = \sqrt{n_0 e^2/m\varepsilon_0} = 5.64\times 10^4 (n_0/\mathrm{cm}^{-3})^{1/2}$ Hz is the background plasma (with density $n$) frequency, $-e$ is the electron charge, $n_0$ is the electron density in unit of $cm^{-3}$. The plasma can sustain a wakefield with amplitude as large as comparable to $n_0^{1/2}$V/cm [5]. If the relativistic effect is taken into account, the maximum amplitude can be even larger. Therefore, laser wakefield can be excited at amplitudes exceeding 1 GV/cm at the plasma density $10^{18}\mathrm{cm}^{-3}$, at which the plasma frequency $\omega_p/2\pi = 9$THz . One of the important applications of such a high-amplitude wakefield is electron acceleration. Recent experiments have demonstrated electron acceleration up to 1GeV within an acceleration distance of few centimeters [55]. Another possible application with the electron plasma wave is the generation of high-amplitude THz emission. Even though the electrostatic plasma wave usually cannot emit, electromagnetic and electrostatic waves can be converted into each other in plasma under certain conditions.

The electron plasma wave at a small amplitude in a uniform plasma is described by $\delta n = \delta n_p \exp[i(k_p x - \omega_p t)]$, where $\delta n_p$ is the electron density perturbation, $k_p = \omega_p/c = 2\pi/\lambda_p$, and $\lambda_p$ is the plasma wavelength. This infinite one-dimensional (1D) plasma wave can never emit electromagnetic waves at frequency $\omega_p/2\pi$ (or wavelength $\lambda_p$), since its displacement current ($\varepsilon_0 \partial \mathbf{E}/\partial t$) exactly compensates for the plasma current ($-en\mathbf{v}$). This means that the wakefield is a pure electrostatic wave. However, there are several ways to make the total wakefield current nonzero. The first is to introduce plasma inhomogeneities. An electromagnetic wave can convert into an electrostatic wave through the so-called linear mode conversion, which leads to the resonance absorption of light in inhomogeneous plasma [56]. Means *et al.* first studied the inverse problem and found that there is a reversal symmetry in the electromagnetic-electrostatic mode conversion [57], which was further confirmed later by Hinkel-Lipsker *et al.* [58]. Simi-

larly, we find that linear mode conversion from the laser wakefield to electromagnetic pulses can occur in certain conditions: the plasma wave is excited in inhomogeneous plasma [19, 20]. The plasma wave in inhomogeneous underdense plasma can be excited by different ways, e.g., by the wakefield of an ultrashort laser pulse or by the beam wave of two co-propagating laser pulses. In the case with the wakefield excitation, usually the plasma wave can be excited in a large region of the inhomogeneous plasma. Mode conversion occurs in the whole region and resulting emission has a large spectrum width. In the case with beat-wave excitation, the plasma wave is excited only in a small region where the local electron plasma frequency equals to the beat-wave frequency.

Another way is to use finite plasma thickness [24]. In this case, at the vacuum-plasma boundaries, there is net transient current produced when the electron plasma wave is excited. With this scheme, one can uniquely generate single-cycle THz pulses.

### 3.1 THz emission from electron plasma waves excited in inhomogeneous plasma

For simplicity, we assume the plasma density increases linearly such as shown in Fig. 1(a), which is underdense for incident laser. An ultrashort intense laser pulse is incident from the left with certain angle $\theta$. If $\theta=0$, there is no electromagnetic emission from the laser wakefield by linear mode conversion since the wave vector of the wakefield coincides with the electric field, while the wave vector of the electromagnetic field is perpendicular to its electric field. In order to treat the oblique incidence, we take the 1D PIC code with the boosting frame scheme [49, 50]. The laser pulse has a sine-square profile

$$a_L=a_0\sin^2[\pi(t-x/c)/T] \quad \text{for } 0\le(t-x/c)\le T.$$

Here $a_0$ is related with the peak laser intensity through $I\lambda_0^2=a_0^2\cdot 1.37\times 10^{18}\mathrm{W/cm^2}\mu m^2$. The pulse enters the left boundary of the simulation box with s-polarization in order to distinguish it easily from the p-polarized emission from the wakefield. We take $a_0=0.5$ and $T=20\tau_0$ with $\tau_0$ the laser oscillation period. For the given laser pulse duration, the laser wakefield is excited around the central frequency $\omega_p/\omega_0\sim\tau_0/T=0.05$. For the linear mode conversion from the wakefield to electromagnetic emission, there is an optimized incident angle for high conversion efficiency at particular frequency $\omega$ [20]. For a linear plasma density profile $n_{0e}=n_0(x/L)$, the emission peak occurs at the angle satisfying

$$\sin\theta=0.68(\omega_{p0}L/c)^{-1/3}\tilde{\omega}^{-1},$$

where $\tilde{\omega}=\omega/\omega_{p0}$ and $\omega_{p0}=4\pi n_0e^2/m_e$. For the plasma parameters $L=200\lambda_0$ and $n_0=0.005n_c$, the optimized incident angle at the particular frequency around $\omega/\omega_0=0.05$ is calculated to be 12.4° [20], where $n_c=m\varepsilon_0\omega_0^2/e^2=1.1\times 10^{21}(\mu\mathrm{m}/\lambda_0)^2\ \mathrm{cm}^{-3}$ is the critical density, beyond which the laser cannot propagate, $\omega_0$ is the laser angular frequency. We take the incident angle of 15° in the following simulation.

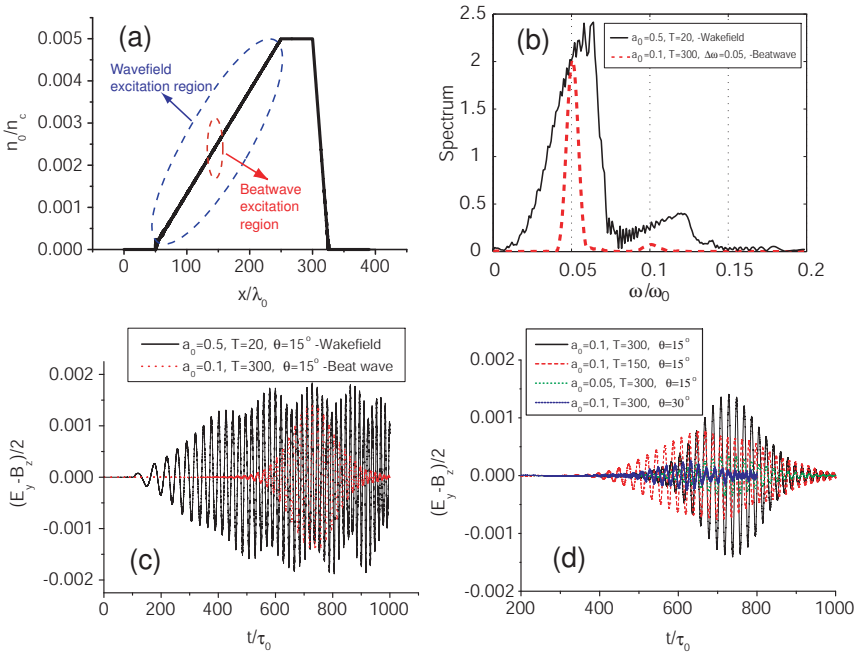


Figure 1: (a) Initial plasma electron density profile (black solid line); The plasma wave excited by laser wakefield distributes in a wide area while that excited by the beatwave of two pulses locates in a particular region where the local plasma frequency is near the beat wave frequency; (b) Emission spectra from the electron plasma wave driven as a wakefield of a short laser pulse and by the beat wave of two laser pulses. In the case of wakefield excitation, the pulse duration and peak amplitude are $T=20\tau_0$ and $a_0=0.5$. In the case of beat wave excitation, two laser pulses have the same duration and peak amplitude $T=300\tau_0$ and $a_0=0.1$, respectively, but with a frequency difference $\Delta\omega=0.05\omega_0$. The laser pulses are incident with the angle of $\theta=15^\circ$; (c) Comparison of the temporal profiles of the THz emission from the laser wakefield and the beat wave with the parameters as in (b); (d) Temporal profiles of the THz emission from the beat wave of two pulses with different parameters.

Figs. 1(b) and 1(c) plot the spectrum and the temporal profile of the emitted pulse. It appears that the emission is peaked near $0.06\omega_0$ with a broad distribution. The reason is that laser wakefied is excited in wide region when the incident pulse is very short as shown in Fig. 2(a). In addition to the fundamental wave, the second harmonic around $0.12\omega_0$ is also observed. This is due to the nonlinear feature of the laser wakefield, which contains harmonic components. The temporal profile of the emission appears as a chirped pulse with its frequency increases with time. This is due to the fact that the emission from the high density region (with relatively higher frequencies) generates at later time and it propagates through a longer distance to the vacuum-plasma boundary. The emission corresponds to a field strength of about 50MV/cm. Figs. 2(a) and 2(b) show the spatial-temporal plots of the longitudinal electric field $E_x$ and magnetic field $B_z$. The latter is concerned with the emitted field. It is found that the wave vector of the electron plasma wave evolves with time and space. In certain time-space region, the wave-vector becomes zero. The linear mode conversion is found when the wave vector $|\mathbf{k}|^2=0$.

Because of the wakefield amplitude is proportional to $a_0^2$, the amplitude of the THz emission is also proportional to $a_0^2$. The energy conversion efficiency can be obtained by

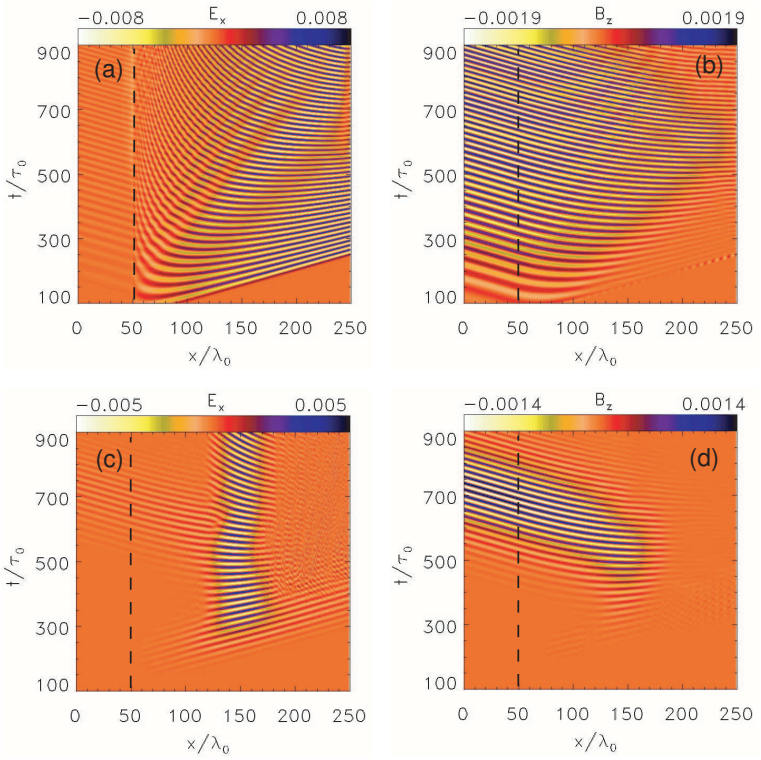


Figure 2: Spatial-temporal plots of the longitudinal electric field $E_x$ and magnetic field $B_z$. Plots (a) and (b) are obtained for wakefield excitation with the pulse duration and peak amplitude are $T=20\tau_0$ and $a_0=0.5$; Plots (c) and (d) are obtained for beat wave excitation, where the two laser pulses have the same duration and peak amplitude $T=300\tau_0$ and $a_0=0.1$, respectively, but with a frequency difference $\Delta\omega=0.05\omega_0$. The laser pulses are incident with the angle of $\theta=15^\circ$ for both cases.

integrating the converted energy in the inhomogeneous region divided by the laser pulse energy. The conversion efficiency can be written approximately as [20]

$$\varepsilon_{energy}\sim C(\tau_0/T)^5(n_c/n_0)(L/\lambda_0)a_0^2,$$

where $C$ is a factor around 1 and is mainly dependent on incident angle $\theta$ and the pulse profile.

Another way to generate high-amplitude electron plasma waves is so-called the beat wave excitation [5], where two co-propagating laser pulses with a frequency difference $\Delta\omega$ comparable to the electron plasma frequency are adopted. In Figs. 1(b) and 1(d), the spectrum and the temporal profile of the emission are plotted under the condition $\Delta\omega/\omega_0=0.05$. The emission has a narrow spectrum as compared with that obtained from the laser wakefield since the electron plasma wave is excited mainly in the localized region with the local frequency $\omega_p\sim\Delta\omega$. This is most obvious from the spatial-temporal plots of the longitudinal electric field $E_x$ and magnetic field $B_z$ as shown in Figs. 2(c) and 2(d).

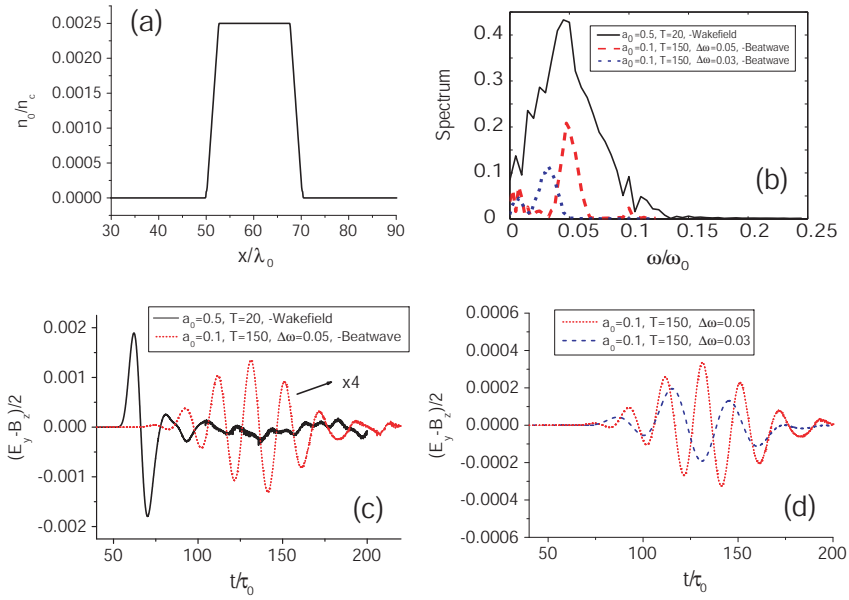


Figure 3: (a) Initial plasma electron density profile; (b) Emission spectra from the electron plasma wave driven as a wakefield of a short laser pulse and by the beat wave of two laser pulses. In the case of wakefield excitation, the pulse duration and peak amplitude are $T=20\tau_0$ and $a_0=0.5$. In the case of beat wave excitation, two laser pulses have the same duration and peak amplitude $T=150\tau_0$ and $a_0=0.1$, respectively, but with a frequency difference $\Delta\omega=0.05$ or $0.03\omega_0$. The laser pulses are incident with the angle of $\theta=60°$; (c) Comparison of the temporal profiles of the THz emission from the laser wakefield and the beat wave with the parameters as in (b); (c) Temporal profiles of the THz emission from the beat wave of two pulses with different frequency difference.

Because of the wakefield amplitude is proportional to $a_{10}a_{20}=a_0^2$, where $a_{10}$ and $a_{20}$ are the amplitudes of the two co-propagating pulses, the amplitude of the THz emission is also proportional to $a_0^2$. The energy conversion efficiency can be obtained by integrating the converted energy in the inhomogeneous region divided by the laser pulse energy. The conversion efficiency can be written approximately as [20]

$$\varepsilon_{energy}\sim C(\Delta\omega/\omega_0)^4(n_c/n_0)a_0^2,$$

where $C$ is a factor mainly dependent on incident angle $\theta$.

### 3.2 THz emission from electron plasma waves excited in a thin plasma layer

A finite wakefield with $L\sim\lambda_p$ (called as a plasma oscillator) can radiate electromagnetic waves for the following reasons. Firstly, for such a few-plasma-wavelength plasma oscillator, its displacement current and real current cannot completely counteract each other, in particular near the plasma-vacuum boundaries. Secondly, since the plasma skin depth of the radiation at frequency $\omega_p$ is simply $k_p^{-1}$, which is comparable to the plasma length $L$. Therefore the radiation can tunnel through the thin plasma layer into vacuum. In order to demonstrate this scheme, we have conducted 1D PIC simulation with the plasma density profile as given in Fig. 3(a). It is found theoretically that THz emission amplitude

scales proportional to $n^{1/2}a_0^2\sin\theta$ [24], which is different from the linear mode conversion. Figs. 3(b) and 3(c) show the spectrum and the temporal profile of the emitted pulse when the electron plasma wave is excited by laser wakefield. We take $a_0=0.5$, $T=20\tau_0$, and the incident angle $\theta=60^\circ$. The emission appears as a single cycle pulse, which implies a broad spectrum. If the electron plasma wave is excited by the beat wave of two laser pulses, multi-cycle emission is observed as shown in Fig. 3(d). Furthermore, if the beat-wave frequency $\Delta\omega=0.03$, which is less than the electron plasma frequency, emission from the plasma oscillation is still observed. The corresponding spectrum is located around this frequency.

Fig. 4 illustrates the spatial-temporal plots for the longitudinal electric field and the transverse magnetic field. It appears that strong longitudinal fields are produced near the plasma-vacuum boundaries. In the case when the electron plasma wave is produced by laser wakefields, single cycle THz emission is produced as shown in Figs. 4(a) and 4(b). Note that there are two pulses emitted with one along the laser propagation direction and another in the specular reflection direction. If the electron plasma wave is excited by the beat-wave of two laser pulses, multi-cycle THz emission is produced as shown in Figs. 4(c) and 4(d). There are also two pulses emitted as in the previous case.

Fig. 5 illustrates snapshots of the longitudinal electric field and the transverse magnetic field found from 2D PIC simulation when a short laser pulse interacts with a thin plasma layer. In order to deal with the oblique incidence of the laser pulse against the plasma surface, the thin plasma layer is tilted by certain angle. Two THz pulses are observed with one along the laser propagation direction and another in the specular reflection direction, as found in 1D PIC simulation.

### 3.3 Effect of external magnetic fields

It is found that a laser wakefield produced in a magnetized plasma [18] can emit through Cerenkov-like radiation, when the applied external magnetic field is perpendicular to the laser propagation direction. In magnetized homogeneous plasma, the wakefield is not purely electrostatic, there exists an electromagnetic component proportional to the strength of the external magnetic field since this magnetic field can produce a transverse velocity or current by the $\mathbf{v}\times\mathbf{B}$ force along the direction perpendicular to the plane formed by the external magnetic field and laser propagation axis.

When the laser wakefield is produced in magnetized inhomogeneous plasma, similar to the unmagnetized case [20], THz emission is produced through the linear mode conversion from the electrostatic wave into electromagnetic waves. In the magnetized plasma, it is the inverse process of the upper-hybrid resonance absorption [59, 60]. In the unmagnetized case, there is the THz emission only when laser is incident obliquely to the density gradient of inhomogeneous plasmas. However, when the plasma is magnetized with the magnetic field perpendicular to the plane formed by the incident laser axis and plasma density gradient, there is the emission for both normal and oblique incidence of laser pulses. By changing the strength and direction of the applied magnetic

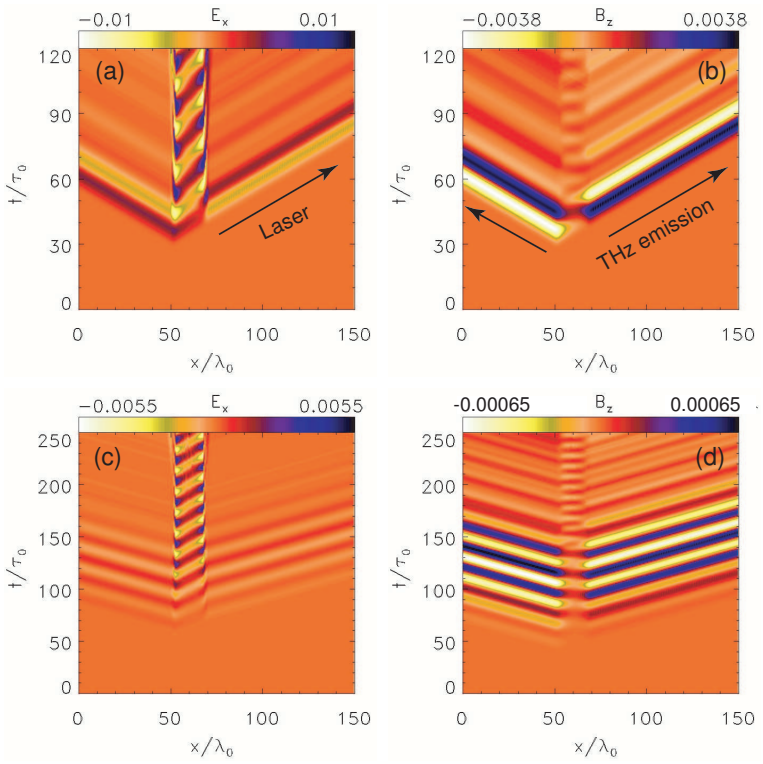


Figure 4: Spatial-temporal plots of the longitudinal electric field $E_x$ and magnetic field $B_z$. Plots (a) and (b) are obtained for wakefield excitation with the pulse duration and peak amplitude are $T=20\tau_0$ and $a_0=0.5$; Plots (c) and (d) are obtained for beat wave excitation, where the two laser pulses have the same duration and peak amplitude $T=150\tau_0$ and $a_0=0.1$, respectively, but with a frequency difference $\Delta\omega=0.05\omega_0$. The laser pulses are incident with the angle of $\theta=60^\circ$ for both cases.

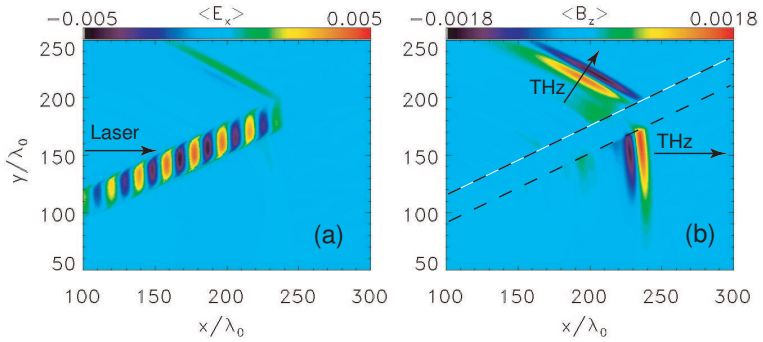


Figure 5: 2D spatial plot of the longitudinal electric field $E_x$ (a) and the pure THz magnetic field $B_z$ (b) from 2D-PIC simulation. The plasma density has a similar profile as in Fig. 3(a) $n=0.0025n_c$, corresponding to $\lambda_p=20\lambda_0$ and $\omega_p/2\pi=14.9$ THz. The plasma length is $L=25\lambda_0$. The laser pulse is $s$-polarized, focused on the plasma slab surface, and has parameters $a_0=0.5$, $T=20\tau_0$, $w_L=30\lambda_0$, and $\theta=60^\circ$. The dashed lines in (b) mark the plasma boundaries, the solid arrows show the THz emission directions, one along the laser propagation and another along the specular reflection direction.

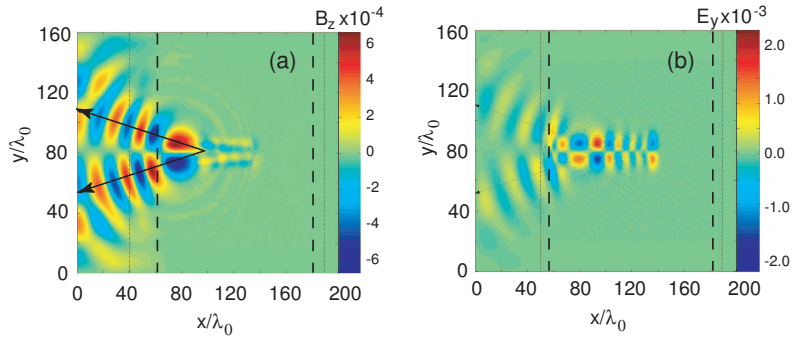


Figure 6: 2D spatial plot of the THz magnetic field $B_z$ (a) and the transverse electric field $E_y$ (b) of the wakefield. The plasma electron density increase linearly from 0 to $0.02n_c$ in a distance of 120 laser wavelengths. The laser pulse is incident normally and is $s$-polarized with parameters $a_0=0.5$, $T=20\tau_0$, $w_L=20\lambda_0$. The Dashed lines mark the plasma boundaries and the solid lines mark the emission direction.

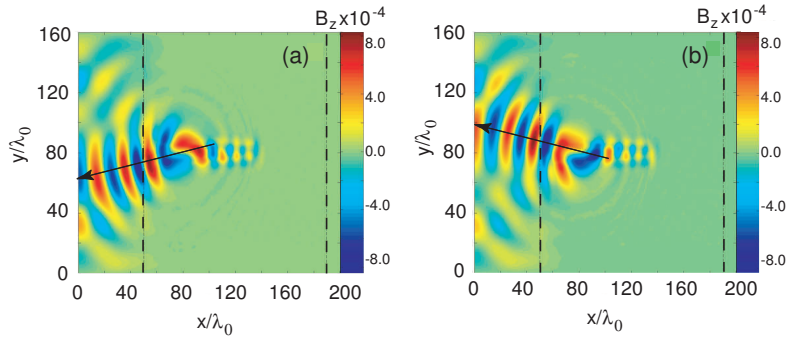


Figure 7: 2D spatial plot of the THz magnetic field $B_z$ . The plasma electron density increase linearly from 0 to $0.02n_c$ in a distance of 120 laser wavelengths. The laser pulse is incident normally and is $s$-polarized with parameters $a_0=0.5$, $T=20\tau_0$, $w_L=20\lambda_0$. An external magnetic field is applied in the z-direction with $B_{z0}=0.007m_e\omega_0 c/e$ (a) and $-0.007m_e\omega_0 c/e$ (b). The Dashed lines mark the plasma boundaries and the solid lines mark the emission directions.

field, one can enhance or suppress the THz emission. The required dc magnetic field is a few tesla (T) [23], lasting for a time scale of tens of picoseconds, which is currently available in many laboratories. The maximum conversion efficiency of the THz emission in the magnetized plasmas can be double that in the unmagnetized case.

The external magnetic field can even change the THz emission direction. To show this we have conducted 2D PIC simulation. Fig. 6 shows snapshots of the transverse magnetic and electric fields when a laser wakefield is produced in inhomogeneous plasma, where the laser pulse propagates along the plasma density gradient. The laser pulse has a finite beam diameter. In Section 3.1, it is pointed out that THz emission is found only when the laser is obliquely incident. In the present case, because of the finite beam diameter, the excited plasma wave has a transverse wave vector, equivalent to the oblique incidence of the laser pulse [20, 21]. In this case, there are two emission peaks around 15° in its backward direction, symmetric to the laser propagation axis. In 3D geometry, it appears as a conical emission. The larger the laser spot diameter, the smaller the emission angle.

On the other hand, if one applies an external magnetic field $B_0 = B_{z0}\hat{z}$ along the z-direction, the emission structure is changed significantly. As shown in Fig. 7(a), the emission becomes collimated along certain direction when a constant magnetic field $B_{z0} = 0.007 m_e \omega_0 c/e$ about 70 Tesla is applied. Moreover, the peak amplitude of the emission is increased as compared to the case without the external magnetic field. If the direction of the magnetic field is reversed, the emission direction is also changed correspondingly, as shown in Fig. 7(b). The effect of the external magnetic field plays a similar role as the incident angle [23]. Note that the required external magnetic field is reduced when the plasma density or the THz frequency decreases. Though the THz field can be increased by a factor of 2 or so as compared to that without the external magnetic field, the scaling of the conversion efficiency with the laser amplitude and plasma density does not change.

# 4 THz emission from gas targets irradiated by short laser pulses

## 4.1 Comparison of THz emission by a single laser and two color lasers

Recently, there are a few experimental studies on THz emission from ionizing air by single pulses or two color lasers (one fundamental and another second-harmonic) [25–28]. It is supposed that the four-wave-mixing (FWM) or optical rectification process may be responsible for the observed emission. However, [28] has noted that the third-order susceptibility index (responsible for FWM) of air is too small to generate the observed THz emission with the field strength greater than kV/cm. Kress *et al.* [26] found that plasma formation is necessary for the THz emission. Meanwhile ionization-induced current models [33, 34] have been proposed to comprehend these THz emissions. These models predict that released electrons by tunneling ionization get transverse momentum while the laser pulse passes. The moving electrons form the THz radiating current, which, however, cannot explain obtained THz pulse frequencies. Here in the following, we present some simulation on THz emission from ionizing gas targets with a single laser or two-color lasers, which may be helpful to understand the experimental observation.

We have used our 2D PIC code to simulate the problem. If one takes gas atoms with many charge states, different ionization states may coexist, which will lead to different emission frequencies at different time during the ionization processes. For simplicity, we only take the Hydrogen gas, which occupies a space of $200\lambda_0$ in the longitudinal direction. Its initial density is $n_{gas} = 1.25\times 10^{-5} n_c$ if not specified in the figure caption. The laser field takes the form

$$a_L = [a_1 \sin(k_0\xi) + a_2 \sin(2k_0\xi + \psi)]\sin^2(\pi\xi/cT_0),$$

where $k_0 = \omega_0/c$, $a_1$ and $a_2$ are the amplitudes for the fundamental and the second harmonic components, respectively, $\psi$ is the phase. The laser is normally incident onto the target. In the following simulation, we take $T = 20\tau_0$. For the two-color case, we keep

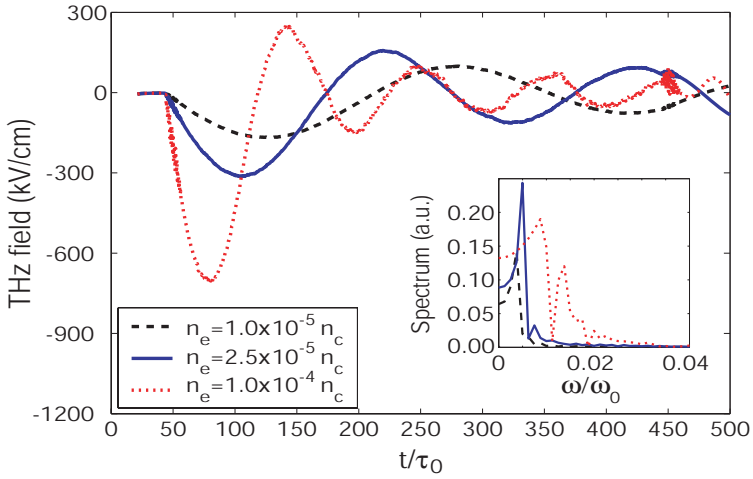


Figure 8: Temporal profiles of the THz emission from a Hydrogen gas target by two-color laser pulses at different densities. The inset shows the corresponding spectra of the emission. The laser peak amplitude is $a_1=0.06$.

$a_2=a_1/2$ and $\psi=\pi/2$. Fig. 8 shows the temporal profiles of the THz emission found at the left boundaries of the simulation box when two-color lasers are adopted. The emission has the same polarization with the incident lasers. We have taken different Hydrogen gas densities so that the final electron densities are at $10^{-5}$, $2.5\times10^{-5}$, and $10^{-4}n_c$. The observed emission frequencies, as shown in the inset of Fig. 8, coincide with the corresponding electron plasma frequencies.

We have found that the observed emission is associated with the ionization processes. Once an electron is released from the atom, its motion is governed by the laser field. For a free electron in a plane wave, we have the motion constant $\mathbf{p}_\perp(t)-e\mathbf{A}_\perp(t)=const.$ [62], where $\mathbf{p}_\perp$ is the transverse momentum of electron, $\mathbf{A}_\perp$ is the transverse vector potential of laser pulse, and $-e$ is the electron charge. At the electron birth time, one has $\mathbf{p}_\perp(t=t_b)=0$. After the laser pulse passes, the field vanishes with $\mathbf{A}_\perp(t=\infty)=0$. From this motion constant, one obtains the final momentum of the electron

$$\mathbf{p}_\perp(t=\infty)=-e\mathbf{A}_\perp(t=t_b),$$

which is determined by the vector potential felt by the electron at the birth time. The last relation is valid when the laser duration is $T\ll\omega_p^{-1}$ and plasma collective response is neglectable. Within the laser pulse, the instant current element is

$$-dn_e(t)e\mathbf{p}_\perp(t)/m=(e^2/m)W_i(t)n_a(t)\mathbf{A}_\perp(t)dt,$$

where $W_i$ is the tunneling ionization rate dependent on the instantaneous electric field $E$, and $n_a$ is the atom density. Integrating it during the pulse duration $0\le t\le T$, we obtain the current density at this space point

$$\mathbf{J}_\perp(\mathbf{r})=\frac{e^2}{m}\int_0^T W_i n_a\mathbf{A}_\perp dt.$$

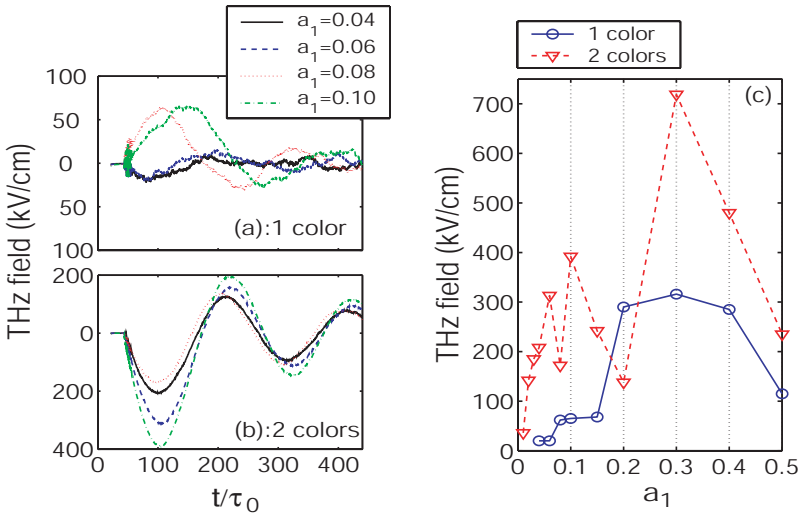


Figure 9: Temporal profiles of the THz emission from a Hydrogen gas target irradiated by two laser pulses at different laser peak amplitudes. (a) With a single laser pulse; (b) With two-color laser pulses; (c) Peak amplitudes of the THz emission as a function of the incident laser amplitude.

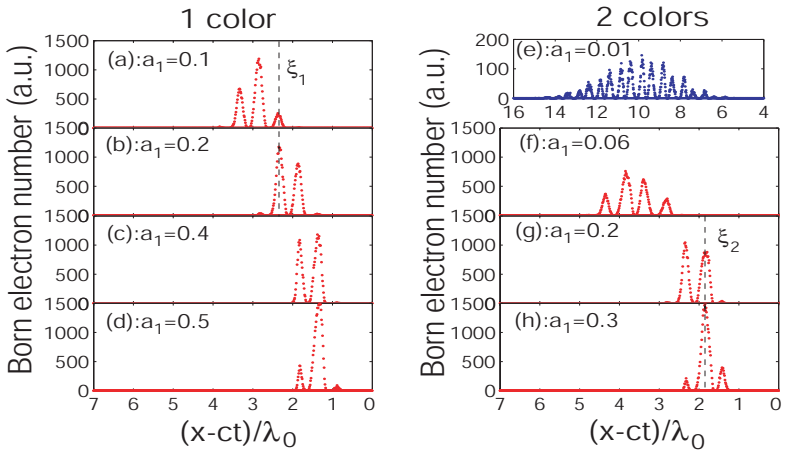


Figure 10: The number of new-born free electrons during the laser interaction within the laser profiles at different laser peak amplitudes. The left and right columns are found for a single laser pulse and two-color laser pulses, respectively.

This current is built up in a very short time $T \ll \omega_p^{-1}$. It radiates THz waves with the central frequency of $\omega_p/2\pi$. The emitted THz amplitudes are the maximum both in forward and backward directions along the light axis [61].

When taking different laser amplitudes, the temporal profiles of the emitted pulses are shown in Figs. 9(a) and 9(b) for a single laser and two-color laser pulses, respectively. For the case with a single laser pulse, the produced net current is noisy and the corresponding emission also shows some noisy features. Even the phases of the emission are different at different incident laser intensities. For the case with two-color laser pulses,

the produced net current appears much larger and the produced emission has the same phase. For $a_1 \leq 0.15$, it appears that the produced THz emission with two-color laser pulses is much stronger than that with a single laser, as shown in Fig. 9(c). In particular, for $a_1 \leq 0.06$, the THz emission amplitude increases with the laser amplitudes of two-color laser pulses, which agrees with experimental results. With the further increase of $a_1$, the THz amplitude changes in a complicated way. This can be explained as follows. At low incident laser intensity, ionization processes occur in many laser periods, and produced net current grows with the peak laser amplitude. At relatively high laser intensity, ionization may occur only in a few laser periods, and the gas may be fully ionized before the laser peak arrives. Therefore, with the further increase of $a_1$, the net current may not increase.

Fig. 10 displays the number of new-born free electrons during the laser interaction within the laser profiles at different laser peak amplitudes. It is obvious that the free electrons are produced over several laser periods when $a_1 = 0.01$. With the further increase of $a_1$, the required laser periods for full ionization is reduced, and the relative position of ionization within the laser pulse envelope is shifted. Therefore, it is not always true that the net current increases with $a_1$.

### 4.2 Conical forward THz emission in ionizing gas targets

Recently the generation of THz emission by laser filaments in air is observed, which is attributed to a combined transition-Cherenkov radiation generated by the space charge created behind the ionization front and moving in the wake of the laser pulse at light velocity [36]. Furthermore, with two laser pulses with certain distance between their centers around the order of $100\mu m$, an enhancement of the THz radiation by more than 1 order of magnitude is observed for time delays shorter than 1 ns between the two pulses. The polarization plane of the THz was determined by the relative position of the two laser filaments. It is explained with a simple model of a transmission line formed by a pair of neighboring plasma filaments [37]. Here in the following, we show some preliminary simulation of such problems.

Fig. 11 shows snapshots of the laser interaction with the Hydrogen gas for the S-polarized laser with $a_0 = 0.02$. From Fig. 11(e) it is found that conical THz emission is produced at the ionization front. The field amplitude is comparable to the longitudinal and transverse electric fields left behind the laser pulse. The result basically agrees with the experimental observation. Fig. 12 shows the simulation with two laser pulses, transversely separated, co-propagating in the gas target. However the result [particularly the emitted pulse as plotted in Fig. 12(e)] is basically the same as for the single pulse case. This means that our simulation at the moment cannot explain the experimental observation [37]. Note that Figs. 11 and 12 are obtained with s-polarized lasers. If the lasers are with p-polarization, emission along the laser propagation axis shown in Fig. 8 is observed.

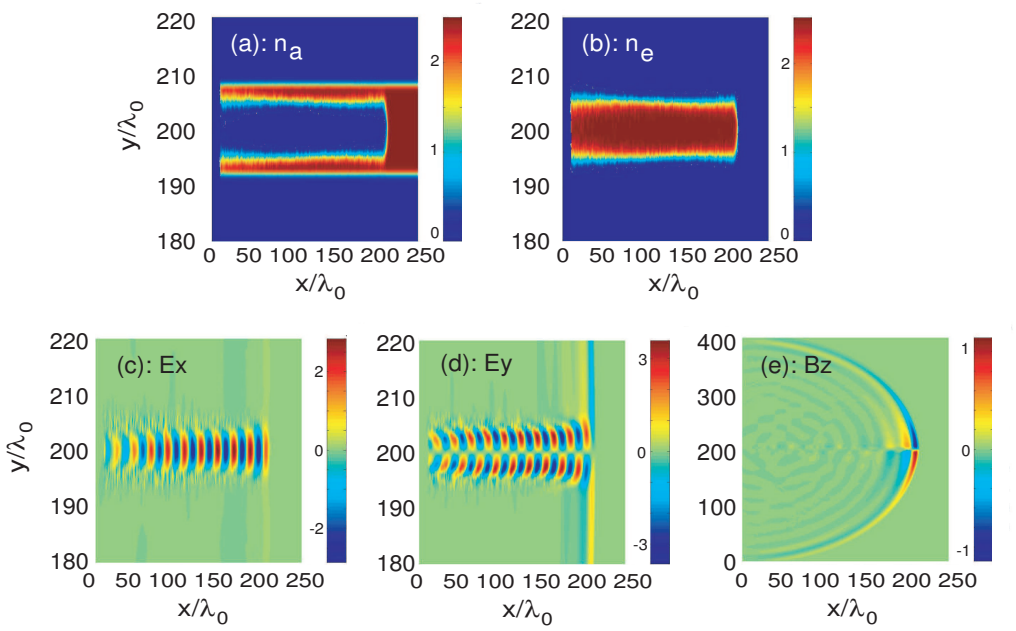


Figure 11: Snapshots of the laser interaction with the Hydrogen gas. The initial atom density is $2.5\times10^{-3}$. The laser is S-polarized and incident with $a_0=0.02$, $T=20\tau_0$, $w_L=10\lambda_0$. (a) The atom density ; (b) The electron density; (c) The longitudinal electric field; (d) The transverse electric field; (f) The transverse magnetic field component, which is just the magnetic component of the THz emission. The densities are multiplied by a factor of $10^3$, and the fields are multiplied by a factor of $10^6$.

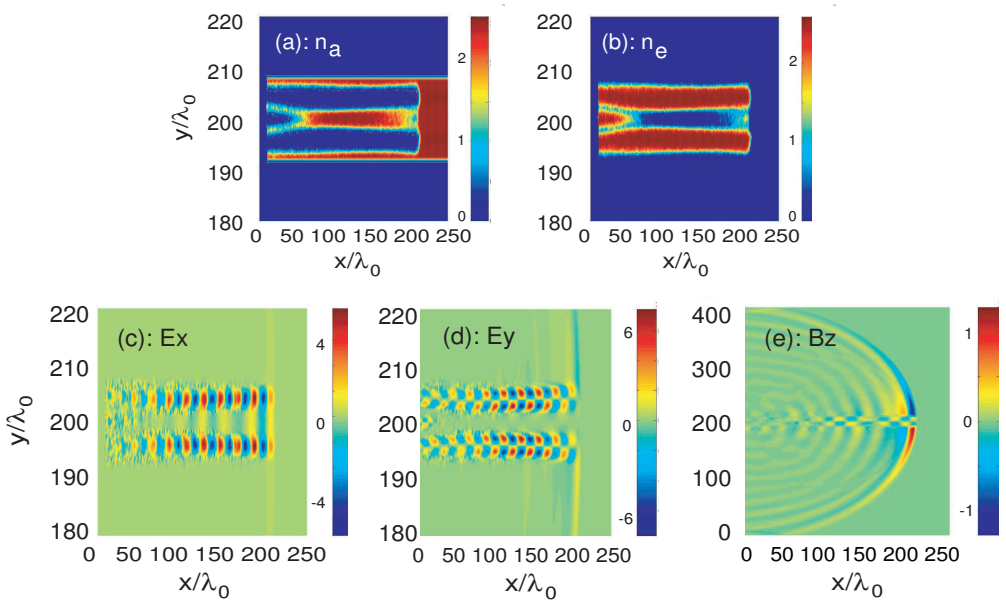


Figure 12: Snapshots of the laser interaction with the Hydrogen gas. The difference from Fig. 11 is that two laser pulses are invoked, which are incident simultaneously with a transverse separation of $16\lambda_0$.

## 5 Summary

By PIC simulation, we have illustrated that high-amplitude electron plasma waves, either driven by laser wakefields or the beatwave of two laser pulses, can emit a powerful THz electromagnetic pulse by means of linear mode conversion in inhomogeneous plasma or by the transient current induced at the surfaces of a thin plasma layer of few plasma wavelengths. With a large size of inhomogeneous plasma, a chirped pulse is produced, while with a thin plasma layer, two single-cycle pulses are produced. An external dc magnetic field of a few tesla, applied in the direction perpendicular to the incident plane of the laser pulse, can change the intensity and direction of the THz emission. The emission frequency, bandwidth, and pulse duration are fully controlled by the incident pulse duration, incident angle, and the plasma density profile. Such plasma-wave emission can be potentially a powerful THz source at tens of MW level and capable of affording field strengths of a few MV/cm, suitable for the studies of THz nonlinear physics.

With field ionization included in the PIC code, we have investigated the THz emission from laser interaction with gas targets. It is found that the transient transverse current formed during the ionization processes is responsible for the THz emission. Our simulation has shown that with two-color lasers, the current can be well-controlled, so that the produced THz field amplitude increases monotonically with the incident laser amplitude within certain regime, which agrees with experimental observation. For the normalized laser amplitude larger than 0.06, the emission amplitude does not show monotonic increase with the laser amplitude. Finally we have simulated THz emission from two co-propagating lasers with certain transverse gap. There is not obvious increase of the THz emission intensity as compared to the case with one laser.

## Acknowledgments

The authors wish to dedicate this article to Prof. X. T. He for celebrating his 70th birthday. ZMS is grateful to Prof. He for his encouragement and support over the last decade. This work was supported in part by the National Natural Science Foundation of China (Grants No. 10425416, 10335020, 10674175, 60621063), the National High-Tech ICF Committee in China, and the National Basic Research Program of China (Grant No. 2007CB310406).

### References

[1] G. A. Mourou, T. Tajima, and S. V. Bulanov, Optics in the relativistic regime, Rev. Mod. Phys., 78 (2006), 309-371.

[2] M. Tabak, J. Hammer, M. E. Glinsky, W. L. Kruer, S. C. Wilks, J. Woodworth, E. M. Campbell, M. D. Perry, R. J. Mason, Ignition and high gain with ultrapowerful lasers, Phys. Plasmas, 1 (1994), 1626-1634.

[3] R. Kodama, P. A. Norreys, K. Mima, A. E. Dangor, R. G. Evans, H. Fujita, Y. Kitagawa, K. Krushelnick, T. Miyakoshi, N. Miyanaga, T. Norimatsu, S. J. Rose, T. Shozaki, K. Shigemori,

A. Sunahara, M. Tampo, K. A. Tanaka, Y. Toyama, T. Yamanaka, and M. Zepf, Fast heating of ultrahigh-density plasma as a step towards laser fusion ignition, Nature, 412 (2002), 798-802.
[4] T.Q. Chang, Y.K. Ding, D.X. Lai, T.X. Huan, S.P. Zhu, Z.J. Zheng, G.Y. Wang, Y.M. Zheng, X.T. He, W.B. Pei, Q.S. Duan, W.Y Zhang, T.G. Feng, G.N. Chen, and P.J. Gu, Laser hohlraum coupling efficiency on the Shenguang II facility, Phys. Plasmas, 9 (2002), 4744-4748.
[5] E. Esarey, P. Sprangle, J. Krall, and A. Ting, Overview of plasma-based accelerator concepts, IEEE Trans. Plasma Sci., 24 (1996), 252-288.
[6] S. V. Bulanov, T. Zh. Esirkepov, F. F. Kamenets, Y. Kato, A. V. Kuznetsov, K. Nishihara, F. Pegoraro, T. Tajima and V. S. Khoroshkov, Generation of high-quality charged particle beams during the acceleration of ions by high-power laser radiation, Plasma Phys. Rep., 28 (2002), 975-991.
[7] C. T. Zhou and X. T. He, Influence of a large oblique incident angle on energetic protons accelerated from solid-density plasmas by ultraintense laser pulses, Appl. Phys. Lett., 90 (2007), 031503.
[8] R. Lichters, J. Meyer-ter-Vehn, and A. Pukhov, Short-pulse laser harmonics from oscillating plasma surfaces driven at relativistic intensity, Phys. Plasmas, 3 (1996), 3425-3437.
[9] W. P. Leemans, E. Esarey, J. van Tilborg, P. A. Michel, C. B. Schroeder, C. Tóth, C. G. R. Geddes, and B. A. Shadwick, Radiation from laser accelerated electron bunches: coherent eerahertz and femtosecond X-Rays, IEEE Trans. Plasma Sci., 33 (2005), 8-22.
[10] M. S. Sherwin, C. A. Schmuttenmaer, and P. H. Bucksbaum, Editors, Opportunities in THz Science, Report of a DOE-NSF-NIH Workshop held February 12-14, 2004, Arlington, VA.
[11] B. Ferguson and X. C. Zhang, Materials for terahertz science and technology, Nature Mater. 1 (2002), 26-33.
[12] M. Tonouchi, Cutting-edge terahertz technology, Nature Photonics, 1 (2007), 97-105.
[13] K. Reimann, Table-top sources of ultrashort THz pulses, Rep. Prog. Phys., 70 (2007), 1597-1632.
[14] G. L. Carr, M. C. Martin, W. R. McKinney, K. Jordan, G. R. Neil, and G. P. Williams, High-power terahertz radiation from relativistic electrons, Nature, 420 (2002), 153-156.
[15] W. P. Leemans, C.G.R.Geddes, J.Faure et al., Observation of terahertz emission from a laser-plasma accelerated electron bunch crossing a plasma-vacuum boundary, Phys. Rev. Lett., 91 (2003), 074802.
[16] H. Hamster, A. Sullivan, S. Gordon, and R. W. Falcone, Short-pulse terahertz radiation from high-intensitylaser- produced plasmas, Phys. Rev. E, 49 (1994), 671-677.
[17] N. Yugami, T. Higashiguchi, H. Gao, S. Sakai, K. Takahashi, H. Ito, Y. Nishida, and T. Katsouleas, Experimental observation of radiation from Cherenkov wakes in a magnetized plasma, Phys. Rev. Lett., 89 (2002), 065003.
[18] J. Yoshii, C. H. Lai, T. Katsouleas, C. Joshi and W. B. Mori, Radiation from Cerenkov wakes in a magnetized plasma, Phys. Rev. Lett., 79 (1997), 4194-4197.
[19] Z. M. Sheng, K. Mima, J. Zhang, and H. Sanuki, Emission of electromagnetic pulses from laser wakefields through linear mode conversion, Phys. Rev. Lett., 94 (2005), 095003.
[20] Z. M. Sheng, K. Mima, J. Zhang, Powerful terahertz emission from laser wake fields excited in inhomogeneous plasmas, Phys. Plasmas, 12 (2005), 123103.
[21] Z. M. Sheng, H. C. Wu, K. Li, and J. Zhang, Terahertz radiation from the vacuum-plasma interface driven by ultrashort intense laser pulses, Phys. Rev. E, 69 (2004), 025401.
[22] Z. M. Sheng, J. Zheng, H. C. Wu, J. Zhang, and K. Mima, Powerful terahertz emission from laser wakefields in plasmas for diagnostics, J. Plasma Phys., 72 (2006), 795-798.
[23] H. C. Wu, Z. M. Sheng, Q. L. Dong, H. Xu, and J. Zhang, Powerful terahertz emission from

laser wakefields in inhomogeneous magnetized plasmas, Phys. Rev. E, 75 (2007), 016407.
[24] H. C. Wu, Z. M. Sheng, and J. Zhang, Single-cycle powerful (MW-GW) terahertz pulse generation from a wavelength-scale plasma oscillator, Phys. Rev. E, 77 (2008), 046405.
[25] D. J. Cook and R. M. Hochstrasser, Intense terahertz pulses by four-wave rectification in air, Opt. Lett., 25 (2000), 1210-1212.
[26] M. Kre$\beta$, T. Löffler, S. Eden, M. Thomson, and H. G. Roskos, Terahertz-pulse generation by photoionization of air with laser pulses composed of both fundamental and second-harmonic waves, Opt. Lett., 29 (2004), 1120-1122.
[27] T. Bartel, P. Gaal, K. Reimann, M. Woerner, T. Elsaesser, Generation of single-cycle THz transients with high electric-field amplitudes, Opt. Lett., 30 (2005), 2805-2807.
[28] X. Xie, J. Dai, and X. C. Zhang, Coherent control of THz wave generation in ambient air, Phys. Rev. Lett., 96 (2006), 075005.
[29] M. Kre$\beta$, T. Löffler, M. D. Thomson, R. Dörner, H. Gimpel, K. Zrost, T. Ergler, R. Moshammer, U. Morgner, J. Ullrich, and H. G. Roskos, Determination of the carrier-envelope phase of few-cycle laser pulses with terahertz-emission spectroscopy, Nat. Phys., 2 (2006), 327-331.
[30] S. Tzortzakis, G. Méchain, G. Patalano, Y.-B. André, B. Prade, M. Franco, A. Mysyrowicz, J.-M. Munier, M. Gheudin, G. Beaudin, and P. Encrenaz, Coherent subterahertz radiation from femtosecond infrared filaments in air, Opt. Lett., 27 (2002), 1944-1946.
[31] J. Kasparian, J.-P. Wolf, Physics and applications of atmospheric nonlinear optics and filamentation, Opt. Exp. 16 (2008), 466-493.
[32] P. Sprangle, J. R. Penano, B. Hafizi, and C. A. Kapetanakos, Ultrashort laser pulses and electromagnetic pulse generation in air and on dielectric surfaces, Phys. Rev. E, 69 (2004), 066415.
[33] K.-Y. Kim, J. H. Glownia, A. J. Taylor, and G. Rodriguez, Terahertz emission from ultrafast ionizing air in symmetry-broken laser fields, Opt. Express, 15 (2007), 4577-4584.
[34] V. B. Gildenburg and N. V. Vvedenskii, Optical-to-THz wave conversion via excitation of plasma oscillations in the tunneling-ionization process, Phys. Rev. Lett., 98 (2007), 245002.
[35] D. H. Auston, K. P. Cheung, J. A. Valdmanis, and D. A. Kleinman, Cherenkov radiation from femtosecond optical pulses in electro-optic media, Phys. Rev. Lett. 53 (1984) 1555-1558.
[36] C. D'Amico, A. Houard, M. Franco, B. Prade, A. Mysyrowicz, A. Couairon, and V. T. Tikhonchuk, Conical forward THz emission from femtosecond-laser-beam filamentation in air, Phys. Rev. Lett., 98 (2007), 235002.
[37] Y. Liu, A. Houard, B. Prade, S. Akturk, and A. Mysyrowicz, and V. T. Tikhonchuk, Terahertz radiation source in air based on bifilamentation of femtosecond laser pulses, Phys. Rev. Lett., 99 (2007), 135002.
[38] M. Chen, Z. M. Sheng, Q.-L. Dong, M.-Q. He, S.-M. Weng, Y.-T. Li, and J. Zhang, Ion acceleration by colliding electrostatic shock waves in laser-solid interaction, Phys. Plasmas, 14 (2007), 113106.
[39] C. Ren, M. Tzoufras, F. S. Tsung, W. B. Mori, S. Amorini, R. A. Fonseca, L.O. Silva, J. C. Adam, and A. Heron, Global simulation for laser-driven MeV electrons in fast ignition, Phys. Rev. Lett., 93 (2004), 185004.
[40] J. M. Dawson, Particle simulation of plasmas, Rev. Mod. Phys., 55 (1983), 403-447.
[41] C.K. Birdsall, A.B. Langdon, Plasma Physics via Computer Simulation, McGraw-Hill, New York, 1985.
[42] A. Pukhov, Strong Teld interaction of laser radiation, Rep. Prog. Phys., 66 (2003), 47-101.
[43] M. Chen, Z. M. Sheng, J. Zheng, Y. Y. Ma, and J. Zhang, Developments and applications of multi-dimensional particle-in-cell codes in the investigation of laser plasma interactions,

Chin. J. Comput. Phys., 25 (2008), 43-50.
[44] T. Zh. Esirkepov, Exact charge conservation scheme for particle-in-cell simulation with an arbitrary form-factor, Comput. Phys. Comm. 135 (2001), 144-153.
[45] T. Umeda, Y. Omura, T. Tominaga, and H. Matsumoto, A new charge conservation method in electromagnetic particle-in-cell simulations, Comput. Phys. Comm., 156 (2003), 73-85.
[46] T. Tajima, Y. C. Lee, Absorbing boundary condition and budden turning point technique for electromagnetic plasma simulations, J. Comput. Phys., 42 (1981), 406-411.
[47] Q. H. Liu, An FDTD algorithm with perfectly matched layers for conductive media, Microwave Opt. Tech. Lett., 14 (1997), 134-137.
[48] Y. Sentoku, private communication.
[49] A. Bourdier, Oblique incidence of a strong electromagnetic wave on a cold inhomogeneous electron plasma, Phys. Fluids, 26 (1983), 1804-1808.
[50] R. Lichters, R. E. W. Pfund, J. Meyer-ter-Vehn, LPIC++ A Parallel one-dimensional relativistic electromagnetic particle-in-cell code for simulating laser-plasma-interaction, MPQ Report 225 (1997), Max-Planck-Institut für Quantenoptik, Garching, Germany.
[51] M. V. Ammosov, N. B. Delone, and V. P. Krainov, Tunnel ionization of complex atoms and of atomic ions in an alternating electromagnetic field, Sov. Phys. JETP, 64 (1986), 1191-1194.
[52] V. Vahedi and M. Surendra, A Monte Carlo collision model for the particle-in-cell method: applications to argon and oxygen discharges, Comput. Phys. Comm., 87 (1995), 179-198.
[53] T. Takizuka, and H. Abe, A binary collision model for plasma simulation with a particle code, J. Comput. Phys., 25 (1977), 205-210.
[54] Y. Sentoku, K. Mima, Y. Kishimoto, and M. Honda, Effects of relativistic binary collisions on PIC simulation of laser plasmas, J. Phys. Soc. Jap., 12 (1998), 4084-4088.
[55] W. P. Leemans, B. Nagler, A. J. Gonsalves, Cs. Tóth, K. Nakamura, C. G. R. Geddes, E. Esarey, C. B. Schroeder, and S. M. Hooker, GeV electron beams from a centimetre-scale accelerator, Nature Phys. 2 (2006), 696-699.
[56] W. L. Kruer, The Physics of Laser Plasma Interaction, Addison-Wesley, New York, 1988.
[57] R. W. Means, L. Muschietti, M. Q. Tran, and J. Vaclavik, Electromagnetic radiation from an inhomogeneous plasma: Theory and experiment, Phys. Fluids 24 (1981), 2197-2207.
[58] D. E. Hinkel-Lipsker, B. D. Frid, and G. J. Morales, Analytical expression for mode conversion of Langmuir and electromagnetic waves, Phys. Rev. Lett. 62 (1989), 2680-2683.
[59] C. Grebogi, C. S. Liu, and V. K. Tripathi, Upper-hybrid-resonance absorption of laser radiation in a magnetized plasma, Phys. Rev. Lett., 39 (1977), 338-341.
[60] W. Woo, K. Estabrook, and J. S. DeGroot, Resonant absorption of laser light by a magnetized plasma, Phys. Rev. Lett., 40 (1978), 1094-1097.
[61] H. C. Wu, J. Meyer-ter-Vehn, Z. M. Sheng, Phase-sensitive terahertz emission from few-cycle laser pulses, New J. Phys., 10 (2008), 043001.
[62] J. Meyer-ter-Vehn, A. Pukhov, and Z.-M. Sheng, in Atoms, Solids and Plasmas in Super-Intense Laser Fields, edited by D. Batani et al. Kluwer Academic/Plenum, Dordrecht, 2001, pp. 167–192.